Michaelis-Menten Kinetics under Spatially Constrained Conditions: Application to Mibefradil Pharmacokinetics

Kosmas Kosmidis,* Vangelis Karalis,† Panos Argyrakis,* and Panos Macheras†
*Department of Physics, University of Thessaloniki, Thessaloniki, Greece; and †Laboratory of Biopharmaceutics-Pharmacokinetics, School of Pharmacy, University of Athens, Athens, Greece

ABSTRACT Two different approaches were used to study the kinetics of the enzymatic reaction under heterogeneous conditions to interpret the unusual nonlinear pharmacokinetics of mibefradil. Firstly, a detailed model based on the kinetic differential equations is proposed to study the enzymatic reaction under spatial constraints and in vivo conditions. Secondly, Monte Carlo simulations of the enzyme reaction in a two-dimensional square lattice, placing special emphasis on the input and output of the substrate were applied to mimic in vivo conditions. Both the mathematical model and the Monte Carlo simulations for the enzymatic reaction reproduced the classical Michaelis-Menten (MM) kinetics in homogeneous media and unusual kinetics in fractal media. Based on these findings, a time-dependent version of the classic MM equation was developed for the rate of change of the substrate concentration in disordered media and was successfully used to describe the experimental plasma concentration-time data of mibefradil and derive estimates for the model parameters. The unusual nonlinear pharmacokinetics of mibefradil originates from the heterogeneous conditions in the reaction space of the enzymatic reaction. The modified MM equation can describe the pharmacokinetics of mibefradil as it is able to capture the heterogeneity of the enzymatic reaction in disordered media.

INTRODUCTION

Michaelis-Menten (MM) kinetics is a basic enzyme kinetics scheme (Michaelis and Menten, 1913), used extensively in chemistry and biology for the study of enzymatic catalysis as it is a relatively simple model from a mathematical point of view. It is of central importance in the field of biotransformation of drugs and is the core of nonlinear pharmacokinetics (Wagner, 1993). The foundation of MM formalism relies on the mass-action law as applied to enzymatic reactions. However, the application of the mass-action law and the derivation of MM kinetics both assume that the substrate-enzyme reaction takes place in a homogeneous medium, i.e., well-mixed, three-dimensional (3D) space and dilute conditions. Although this assumption is usually satisfied under in vitro conditions, the complexity of biological media makes it questionable when MM kinetics is considered under in vivo conditions. Indeed, various reports indicate that cellular media are structurally heterogeneous (Scalettar et al., 1991; Minton, 1993, 1998; Luby-Phelps et al., 1987; Frauenfelder et al., 1999) and this has an impact on the validity of Fick's law of diffusion in living cells (Agutter et al., 1995). The reason is (see Berry, 2002 and references therein) that diffusion depends on the Euclidean dimension d of the medium in which it occurs. For a medium with $d > 2$, a diffusing molecule explores only a low fraction of the accessible volume and thus it always escapes its initial position (noncompact diffusion). For a medium with $d < 2$, the molecule eventually returns to its initial position with probability 1 (compact diffusion) and thus diffusion is not a perfectly mixing process in low dimensions (Montroll and Weiss, 1965). This has important consequences on the mean-squared displacement of the molecule, which scales with time as $\langle R^2 \rangle \propto t^n$. The exponent $n = 1$ denotes Fickian diffusion whereas $n < 1$, observed in many low-dimensional media, denotes anomalous diffusion. Nonclassic diffusion has been observed in cellular media for water (Köpf et al., 1996), and fluorescence probes (Schwille et al., 1999; Wachsmuth et al., 2000). In general, many cellular reactions take place under dimensionally restricted conditions, e.g., two-dimensional (2D) membranes, quasi-one-dimensional tubes or other disordered media. This type of reaction has been found to exhibit noninteger kinetic orders in in vitro experimental studies (Sadana, 2001; Ramakrishnan and Sadana, 2002) and in simulation (Koo and Kopelman, 1991), rather than the usual integer kinetic order derived from mass-action kinetics. These noninteger kinetic orders are related to the fractal dimension of the space in which the reaction occurs; therefore, the nonconventional kinetics have been referred to as ''fractal kinetics'' (Kopelman, 1988). Typically when power-law behavior is observed, this is manifested in a log-log plot with a straight line section. At short times the system is still not equilibrated enough and as this regime is amplified by the log-log plotting, a straight line is not observed. This happens only when the system has the chance to reach some sort of equilibrium and this usually happens at long times.

In this context, theoretical approaches (López-Quintela and Casado, 1989; Berry, 2002; Savageau, 1998) based on fractal principles have been used to describe enzyme kinetics in low-dimensional disordered media. One of these approaches (López-Quintela and Casado, 1989) has been also used to interpret experimental data of carrier-mediated

Submitted March 8, 2004, and accepted for publication May 20, 2004.
Address reprint requests to Panos Argyrakis, E-mail: panos@physics.auth.gr.

0006-3495/04/09/1498/09 $2.00
doi: 10.1529/biophysj.104.042143

transport (Macheras, 1995; Ogihara et al., 1998). It is proposed that the liver is a fractal-like object. In fact Javanaud (1989), using ultrasonic wave scattering, has measured the fractal dimension of the liver as approximately $d_f \approx 2$ over a wavelength domain of 0.15–1.5 mm. Recently, Fuite et al. (2002) proposed that the fractal structure of the liver with attendant kinetic properties of drug elimination can explain the unusual nonlinear pharmacokinetics of mibefradil (Skerjanec et al., 1996; Welker, 1998). In this work we study the effect of species segregation on the kinetics of the enzyme reaction, firstly by using a microscopic pharmacokinetic model, and secondly by carrying out Monte Carlo (MC) simulations mimicking the intravenous (i.v.) and per os (p.o.) administration of the substrate for an enzyme reaction taking place in fractal media. The substrate profiles generated from both approaches were found to be in accord with mibefradil experimental observations. Based on these findings we developed a modified MM equation incorporating the time dependence in the Michaelian ''constant,'' and we further used it to interpret the unusual nonlinear pharmacokinetics of mibefradil (Fuite et al., 2002; Skerjanec et al., 1996; Welker, 1998) at the macroscopic level. We would like to emphasize that the models presented below represent only one possible explanation for reactions occurring in disordered media and they are certainly not the only possible approach.

METHODS

The MM model of enzyme kinetics consists of three elementary chemical reactions:

$$E + S \underset{k_{-1}}{\overset{k_1}{\rightleftarrows}} C \overset{k_2}{\rightarrow} E + P, \tag{1}$$

where E, S, P, and C represent the enzyme, substrate, product, and enzyme-substrate complex, respectively, and k_i is the rate coefficient associated with the elementary step i.

Because, after an initial prestabilized period, the concentration of the complex *(C)* in Eq. 1 remains practically constant, a quasistationary state assumption is used for simplification purposes (Wagner, 1993). This simplification allows the derivation of the classic MM Eq. 1:

$$v = \frac{v_{max} p_S}{K_M + p_S}, \tag{2}$$

where v and v_{max} refer to reaction and maximum reaction rate, respectively, p_s is the substrate concentration whereas the term K_M represents the MM constant that is related to the kinetic constants of the reaction scheme (Eq. 1) as follows:

$$K_M = (k_2 + k_{-1})/k_1.$$

Mathematical formulation of a microscopic reaction model of MM kinetics under in vivo conditions

To model the above reaction scheme (Eq. 1) under in vivo conditions we have to take into account that the substrate (drug) is not confined at the reaction medium (liver), but it arrives at the liver either from the portal vein (oral administration) or through circulation (intravenous administration); a part of the substrate is metabolized (Fig. 1) while the rest exits from the liver and returns later through circulation, and so on.

We propose a reaction model that incorporates this fact, without, however, dealing in detail with the drug partition between the blood and the liver, by making the assumption that the substrate molecules that exit from the liver at time t will return to it some time later. We also assume that this time of delay is not constant, but it follows a Gaussian distribution with mean T and variance σ^2. We further assume that E and C remain inside the liver and that only P and S get out and return through the circulatory system. Thus, the mathematical model for the in vivo MM reaction takes the form:

$$\frac{dp_C}{dt} = -\frac{dp_E}{dt} = k_1 p_E p_S - (k_{-1} + k_2) p_C \tag{3}$$

$$\frac{dp_S}{dt} = -k_1 p_E p_S + k_{-1} p_C + RS_{ext}(t) - a_1 p_S + \int_{u=0}^{u=t} a_2 p_S(u) \frac{e^{\frac{-((t-(u+T))^2}{2\sigma^2}}}{\sqrt{2\pi}\sigma} du \tag{4}$$

$$\frac{dp_P}{dt} = k_2 p_C - a_1 p_p + \int_{u=0}^{u=t} a_3 p_p(u) \frac{e^{\frac{-((t-(u+T))^2}{2\sigma^2}}}{\sqrt{2\pi}\sigma} du, \tag{5}$$

where p_i is the concentration of species i at time t. Eqs. 4 and 5 represent modifications of the classic system of ordinary differential equations used to describe the MM scheme. The extra terms that have been added in Eqs. 4 and 5 are listed below along with their physical meaning:

1. $RS_{ext}(t)$ in Eq. 4 is the arrival rate of S to the liver from the gastrointestinal tract. It depends on the way the drug enters the circulatory system at the liver area, and may have the following forms:
   - i.v. bolus injection: $RS_{ext}(t) = 0$ and the system of Eqs. 3–5 has to be solved with the initial condition $p_s(t = 0) = S_0 > 0$.
   - Zero-order input: $RS_{ext}(t) = k_0$ for $t \leq T_a$ and 0 for $t > T_a$, where k_0 is a constant and T_a is the duration of input from the gastrointestinal (GI) tract. The system of Eqs. 3–5 has to be solved with the initial condition $p_s(t = 0) = 0$.
   - First-order input: $RS_{ext}(t) = k_\alpha \times X_0 \times e^{-k\alpha \cdot t}$ where X_0 is a constant quantity (initial concentration of drug in the GI) and k_a is the first-order rate constant. Again the system of Eqs. 3–5 has to be solved with the initial condition $p_s(t = 0) = 0$.

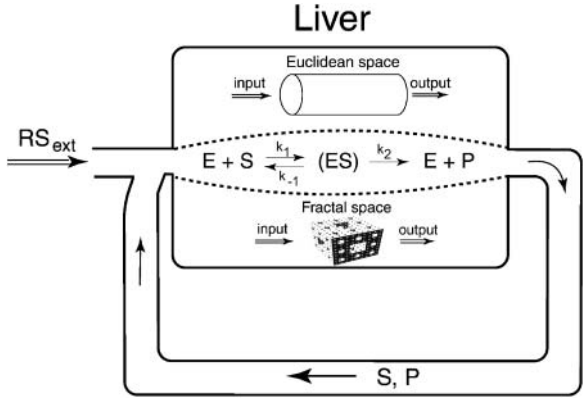

FIGURE 1 A microscopic model for the enzymatic reaction in the liver. The topology of the reaction space in the liver can be considered either Euclidean or fractal. RS_{ext} denotes the rate of substrate input.

2. $-a_1 p_S$ in Eq. 4 is the rate of exit of drug molecules.
3. $\int_{u=0}^{u=t} a_2 p_S(u)(e^{-((t-(u+T))^2/2\sigma^2)}/\sqrt{2\pi}\sigma)du$ in Eq. 4 models the reentrance of drug due to the circulation. The term $a_2 p_S(u)$is the number of drug molecules that exit at time u and the other term is the probability that a drug molecule that exits at u will return at the liver at time t. We integrate to account for the contribution from all times $0 < u < t$.
4. $-a_1 p_p$ in Eq. 5 is the rate of exit of product molecules.
5. $\int_{u=0}^{u=t} a_3 p_p(u)(e^{-((t-(u+T))^2/2\sigma^2)}/\sqrt{2\pi}\sigma)du$ in Eq. 5 models the reentrance of product due to the circulation.

The above system of integro-differential equations becomes even more complicated as we have to take into consideration segregation effects that will arise if we consider some degree of disorder in the medium. The basic fractal kinetics assumption, which is supported by Monte Carlo simulations (Kopelman, 1988; Berry, 2002; Kosmidis et al., 2003b), is that segregation effects arising due to the fractal structure (in this case, the liver) can be incorporated in the model if we assume that k_1, a_1,and a_2 are not constant but follow a power law. Thus, in the above model:

$$k_1 \rightarrow \frac{k_1}{t^{b}}, a_1 \rightarrow \frac{a_1}{t^{m}}, a_2 \rightarrow \frac{a_2}{t^{m}}. \quad (6)$$

In all results presented below, we have, for simplicity, assumed that $\alpha_3 = 0$, i.e., that the product molecules that exit the liver area do not return to it. Because the quantity we are primarily interested in is the blood concentration p_s of substrate in the liver region this will not change the results of the numerical solutions. It may, however, make a difference in the Monte Carlo simulation results for p_s at long times.

Monte Carlo simulations of enzyme reaction in fractal media

We simulated the Michaelis-Menten reaction depicted in Eq. 1 using a 2D square lattice and the Monte Carlo algorithm described below. See Fig. 2 for a graph of a 50 × 50 percolation fractal. Each molecule type performs a random walk on the lattice with excluded volume interactions. To model the complexity of the environment we have two choices, both of them very well known from percolation theory. Either we simply introduce immobile obstacles at a given concentration, c_b, and force particles to move anywhere on the lattice but not on the obstacle sites, or we first introduce immobile obstacles at a given concentration c_b and then we use a cluster labeling technique (as, e.g., the one proposed by Hoshen and Kopelman (1976)) to identify the largest cluster and allow the reaction to occur only at the largest cluster. The largest cluster at the percolation threshold is known as the percolation fractal. Below we will refer to the first model as the ''all-clusters model'' and to the second as the ''largest-cluster model.'' Both models will produce statistically the same results at low concentrations of obstacles, but will differ at long times if the concentration of obstacles is high and the enzyme concentration is low. The reason is that every site of the ''largest cluster'' is connected to every other site, whereas in the ''all-clusters model'' there are also several smaller ''islands,'' where there may be some substrate molecules but no enzyme molecules can access them. Of course these small ''islands'' may be interpreted as areas where the MM reaction is more difficult to occur and both models may lead to useful results. Obviously, when no obstacles are used, then the matrix represents a Euclidean space with dimensionality equal to two. It should be noted that the ''largest-cluster model'' has been used in the past in problems related to drug release from polymeric devices (Bonny and Leuenberger, 1991, 1993; Kosmidis et al., 2003a,b). The ''all-clusters model'' on the other hand was recently used by Berry (2002) for simulating enzyme reactions in restricted geometries.

FIGURE 2 A 50 × 50 percolation fractal. Only the largest cluster is shown. Particles are allowed to move on the white sites only. Black sites are restricted area obstacles. Substrate molecules enter to the lattice from randomly chosen white sites labeled as entrances.

Although the liver is a 3D organ we utilize here a 2D model. This is mainly due to simplicity, especially because both a 2D and a 3D percolation cluster at criticality have the same spectral dimension. This exponent d_s characterizes the area visited by a random walker in a medium. A 2D lattice has $d_s = 2$, whereas a disordered lattice (percolation fractal) has a spectral dimension $d_s \sim 1.34$, both in 2D and 3D lattices (Argyrakis et al., 1993). By inserting immobile obstacles in a 2D lattice and varying their concentration we are able to control the spectral dimension of the medium in a continuous way from 2 to 1.34. The value of the spectral dimension of the liver given by Fuite et al. (2002) is $d_s \sim 1.84$, which is within the above interval (1.34–2.50) and in agreement with our proposed picture. Actually, it was possible to fit the same experimental data as Fuite with our 2D model and produce a better more accurate fit. Thus, using a 2D model per se, is not misleading or questionable.

To mimic the enzyme reaction under in vivo conditions, special emphasis is given to the input and output of the substrate and the output of the product. To this end, we introduce sites that function as exits with a concentration c_{out} and sites that function as entrances with a concentration c_{in}, (see Fig. 2). In all cases presented below (unless otherwise denoted) we have used a 100 × 100 lattice with $c_{in} = 0.3$ and $c_{out} = 0.1$.

Reaction-diffusion processes are usually simulated using a random-walk model. To model a Michaelis-Menten type of reaction, which is actually a set of three elementary reactions (see Eq. 1) we have to introduce three reaction probabilities f, r, and g. These probabilities are proportional to the rate coefficients k_1, k_{-1}, and k_2 (see below and also Berry, 2002). To mimic i.v. bolus injection-type delivery of the drug, at the beginning of each simulation, the E and S molecules are randomly placed on the permissible clusters of the lattice.

To mimic first-order drug delivery we calculate the number of substrate molecules N_{ext} that enter the liver, through the GI tract, from time t until $t + 1$ using the relation $N_{ext}(t) = \int_t^{t+1} k_a X_0 Exp(-k_a t)\, dt$, where X_0 is the initial quantity of drug in the GI and k_a is the first-order rate constant. In simulations using the ''largest-cluster'' model we set the substrate concentration c_s at a constant value and we set $X_0 = c_s\, l_f$, where l_f is the size of the percolation fractal. (For a 100 × 100 lattice the average size of the percolation fractal is a little more than 2500 sites). Those X_0 molecules are gradually placed at the percolation fractal. At each MCS we place N_{ext} substrate molecules around the sites labeled as entrances.

At each MC step, an occupied lattice site is chosen at random (excluding obstacle sites). The rules for movement and reaction depend on the nature of the selected molecule:

1. If the selected molecule is an S, a destination site is chosen at random from its four nearest neighbors. If the destination site is unoccupied, the molecule moves to it directly. If the destination site is occupied by an E molecule, a random number is chosen between 0 and 1. If this number is lower than the reaction probability f, the destination site is turned to a C

molecule and the initial S site becomes unoccupied. In all other cases, the S molecule remains at its initial position. Note that this is also valid if the chosen destination site is an obstacle.

2. If the selected molecule is an E, the process is similar to case 1, i.e., depends on the occupancy status of the randomly chosen destination site. There is a movement if unoccupied, whereas there is a reaction with a probability f if occupied by S, or there is no change in all other cases.
3. If the selected molecule is a C, a random number is chosen between 0 and 1. If this number is lower than the reaction probability r then the C molecule dissociates into an E and an S. The new E molecule is placed on the initial C site, whereas for the new S molecule we choose a site at random. If the site is occupied we abort the decomposition process. The initial C molecule dissociates into an E and a P in a similar fashion, if the random number is $>r$ but lower than $r + g$. Finally, if the random number is greater than $r + g$, the C molecule is allowed to move to a randomly chosen unoccupied nearest neighbor site.
4. If the chosen molecule is a P, it moves to a randomly chosen unoccupied nearest-neighbor site.
5. Sites marked as exits function as block sites for E and C molecules. This accounts for the fact that the enzyme and substrate molecules are not allowed to exit from the liver area. On the other hand a P molecule that meets an exit site is permanently removed from the system.
6. If an S molecule moves to an exit site at time t, a random number x is drawn from a Gaussian distribution with mean τ and standard deviation σ. This particle will return to the system at time $t + x$ and it will be placed at a randomly chosen nearest neighbor of an entrance site.

After each particle move time is incremented by $1/N$, where N is the current number of molecules on the lattice. One time unit thus statistically represents the time necessary for each molecule to move once. The simulation goes on until a prescribed total time is reached. We average our results over 50 realizations for statistical purposes.

RESULTS AND DISCUSSION

Microscopic modeling and MC Simulations

In Fig. 3 we present a plot of p_S versus time based on the numerical solution of the microscopic reaction model and subsequent fitting to the experimental in vivo data (also shown in the plot) using a Levenberg-Marquardt nonlinear fitting algorithm (Press et al., 1988). The fitted line describes the experimental data nicely. Notice the hump around $t = 50$ min, which is predicted from the model and also observed experimentally. It is due to the fact that the drug molecules that exit from the liver return to it after some time, thus temporally increasing p_s, which subsequently is decreased again due to the continuous exiting of substrate particles from the system. The estimates of the parameters (in arbitrary units) of the system of Eqs. 3–6 are: $p_s(0) = 0.3$, $p_e(0) = 0.05$, $k_1 = 1$, $k_{-1} = 0.02$, $k_2 = 0.09$, $a_1 = 0.0302$, $a_2 = 0.0305$, $\tau = 48$, $\sigma = 10$, $b = 0.39$, $m = 0.07$. The correspondence of arbitrary time and density units to the actual units is also determined by the Levenberg-Marquardt and it is found that 1 arbitrary density unit corresponds to 477.99 ng/mL and that 1 arbitrary time unit corresponds to 1.07 min. Particular emphasis should be placed on the estimate $b = 0.39$ for the power-law exponent of ''segregation'' term k_1/t^b (in Eq. 6) because it indicates a reaction taking place at a highly disordered environment.

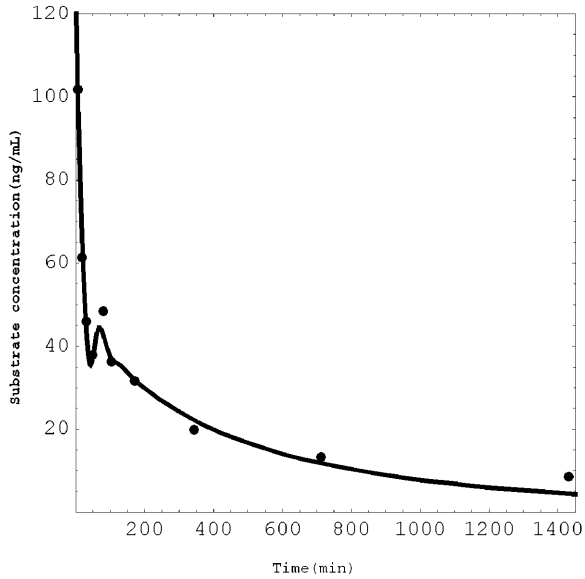

FIGURE 3 Plot of p_S versus time using the microscopic model of the enzymatic reaction. Points are experimental in vivo data from Fuite et al. (2002). The solid line represents results of the numerical solution of the system of Eqs. 3–5 assuming fractal kinetics (i.e., Eq. 6) combined with a Levenberg-Marquardt fitting algorithm. The fitted results are rescaled to change to actual units. Rescaling factors are also determined by Levenberg-Marquardt fitting.

This result is in good agreement with the results of Berry (2002) who also found that k_1 is in essence a time-dependent coefficient in topologically constrained media. It is also interesting to note that the estimate for m was found to be close to zero ($m = 0.07$), which indicates that both the exit and reentrance of the drug are governed by typical rate constants a_1 and a_2, respectively, Eq. 6.

To check the validity of the MC simulations in Fig. 4 we plot p_S versus time for several different enzyme concentrations (p_E) assuming that no obstacles are present, which is a case of normal Euclidean space. We assume i.v. bolus injection delivery of the drug. So all drug molecules are placed at the 2D matrix at random positions at time $t = 0$. The values assumed for the reaction probabilities are $f = 1$, $r = 0.02$ and $g = 0.04$, and $p_s(0) = 0.2$. The results indicate that the substrate concentration decreases exponentially at long times, which is the classically expected behavior anticipated from the Michaelis-Menten reaction scheme in saturated conditions (Wagner, 1993). The condition for this exponential decrease is $Km \gg p_s$, i.e., when the substrate concentration becomes much less than the Michaelis constant (Murray, 1993).

Fig. 5 is a semilog plot of the Monte Carlo simulation data for p_S versus time assuming delivery of the drug through first-order kinetics. We have assumed a fractal structure using the largest-cluster model. The values assumed for the reaction probabilities are $f = 1$, $r = 0.02$, and $g = 0.04$ and the initial enzyme concentration was set to $p_e = 0.06$. All lines represent simulation results. Notice the reaction

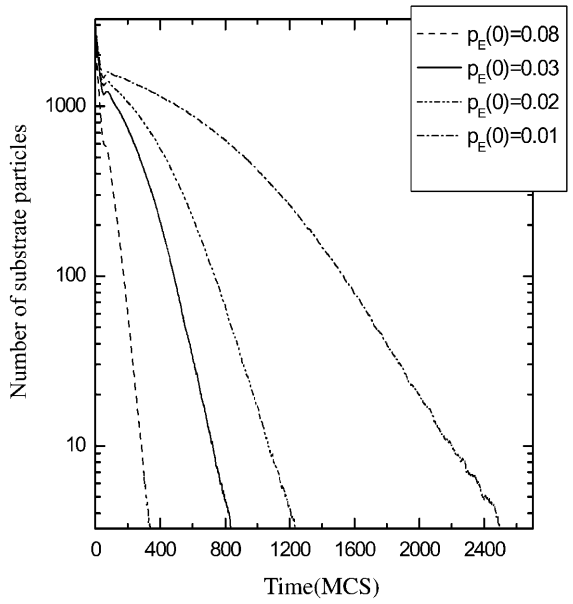

FIGURE 4 Semilog plot of p_S versus time for several initial values of enzyme concentration, p_E, in a Euclidean space (zero density of obstacles) using MC simulation. We assume injection-type drug delivery, i.e., at $t = 0$ all drug molecules are supposed to be in the lattice, randomly distributed. The values assumed for the reaction probabilities are $f = 1$, $r = 0.02$, and $g = 0.04$. The initial substrate concentration was set to $p_s = 0.2$.

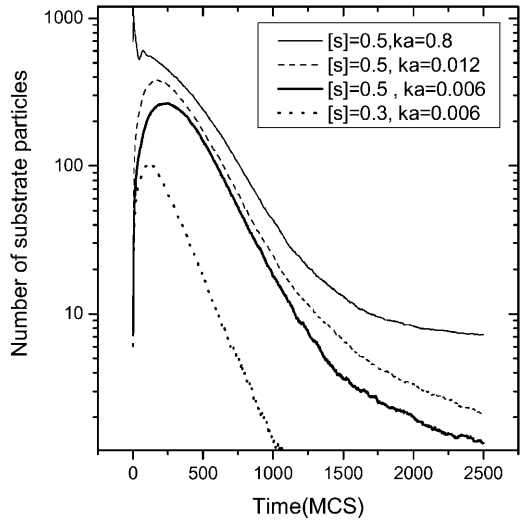

FIGURE 5 MC simulations using the ''largest-cluster model''. Semilog plot of p_S versus time assuming delivery of the drug through first-order kinetics for several values of the first-order constant, k_a, and two levels of the initial substrate concentration. The values assumed for the reaction probabilities are $f = 1$, $r = 0.02$, and $g = 0.04$ and the initial enzyme concentration is $p_e = 0.06$.

slowdown (slope change) at large times in contrast to the classical behavior presented in Fig. 4. This can be interpreted as an indication of ''fractal'' instead of classical kinetics. High values of the first-order rate constant k_a approximate injection delivery whereas low values of k_a mimic slow oral drug input. Experimental results (see also discussion of Fig. 7) show that a high k_a value exhibits a deviation from the classically expected Michaelis Menten behavior, but this is not observed in the oral administration of drug. Simulation results shown in Fig. 5 indicate that high k_a values lead to higher initial drug concentration and to ''fractal kinetics'' (Berry, 2002) behavior whereas this effect is not so obvious for low k_a values. In fact, fractal kinetics is completely masked for the simulations with low initial substrate concentration and low value of k_a.

In all Monte Carlo simulations that monitor the time evolution of a system the time unit of the simulation is 1 Monte Carlo step (MCS). The correspondence of this time unit to the actual time units used in the experimental measurements is determined by a nonlinear fitting and is found that 1 MCS corresponds to 0.88 min.

In Fig. 6 we present a plot of p_S versus time based on the Monte Carlo method. Points are the experimental in vivo data from Fuite et al. (2002), same as in Fig. 3. The dashed line is the MC simulation result using the ''all-clusters model'' and the solid line is the MC result using the ''largest-cluster model.'' We performed several simulations under different conditions. In all cases, to achieve the best possible fitting, we had to assume a fractal structure for the liver either by assuming a concentration of obstacles near the percolation threshold in Monte Carlo simulations or by assuming a power-law form for the ''constants'' as in Eq. 6 in the mathematical modeling. Visual inspection of Fig. 6 reveals that the MC results derived from the ''all-clusters model'' describe better the experimental data than the ''largest-cluster model.'' Any attempt to explain the experimental results using the classical Michaelis-Menten was completely unsatisfactory.

Development and application of an MM equation with time-variant K_m

In addition to the detailed mathematical model that we have presented above, we would like to provide a simpler, approximate, treatment of the problem, which is much easier to use in practical applications.

An algebraic manipulation of the system of Eq. 3–6, using the classical quasistationary assumption and the additional assumptions that α_1, α_2 are small compared to k_1 and that in most cases $RS_{ext}(0)$ is also small, implies that a time-variant K_M will be a suitable approximation. In fact, the above analysis indicates that a power-law form is probably the most appropriate for the time-variant K_M as follows: $K_M = K_{M0} \cdot t^h$, where h is a dimensionless exponent and K_{M0} is a constant expressed in concentration (time)$^{-h}$ units. Under homogeneous conditions, the terms K_M and K_{M0} become identical and express the classic Michaelis constant since $h = 0$. Using the time-variant expression of K_M, the time-dependent version of MM kinetics can be formulated as:

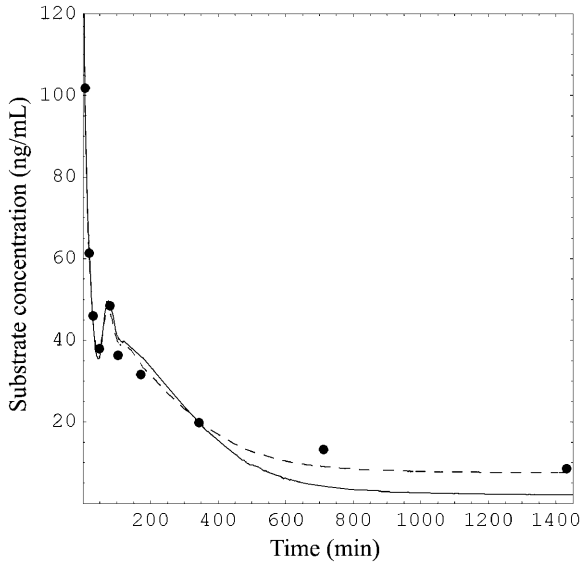

FIGURE 6 Plot of p_S versus time. Points are experimental in vivo data from Fuite et al. (2002). Dashed line represents MCS results using the ''all-clusters model''. The values assumed for the reaction probabilities are $f = 1$, $r = 0.02$, and $g = 0.04$. The following parameters have given the best fitting results: $p_s(0) = 0.2$, $p_e(0) = 0.2$, $T = 48$, $\sigma = 12$. Thin solid line represents MCS results using the ''largest-cluster model''. The following parameters have given the best fitting results: $f = 1$, $r = 0.015$, $g = 0.02$, $ps(0) = 0.6$, $p_e(0) = 0.2$, $T = 48$, $\sigma = 10$. We rescale to change from Monte Carlo units to actual time units. Rescaling factors are determined by Levenberg-Marquardt fitting. In both cases it turns out that 1 min = 0.88 MC steps.

$$v = \frac{v_{max} p_S}{K_{M0} t^h + p_S}. \quad (7)$$

Equation 7 reveals that the rate of the enzyme reaction depends on p_s and t. This time dependency of K_M ($K_M = K_{M0} \times t^h$) leads to an increase of this term with time (depending also on the value of the exponent, h). This characteristic constitutes the underlying cause for the successful application of Eq. 7 to mibefradil data.

Assuming one-compartment model disposition (Wagner, 1993), Eq. 7 was used to analyze the concentration-time data of mibefradil after i.v. and per os administration (Fuite et al., 2002; Skerjanec et al., 1996; Welker, 1998). For comparative purposes the classic Eq. 2 was also used to analyze the same data. Since Eqs. 2 and 7 were applied to concentration-time data (Fuite et al., 2002), the term v_{max} was substituted with v^*_{max} denoting the normalized maximum rate, in terms of the volume of distribution of the compartment. These appropriately modified Eqs. 2 and 7 were fitted to experimental data (Fuite et al., 2002; Skerjanec et al., 1996; Welker, 1998) using a program developed in FORTRAN for the numerical solution of the differential equations. A Levenberg-Marquardt algorithm was utilized for the optimization process. To compare the utilized models as for their ability to successfully describe the data, the Akaike information criterion (AIC), and the Schwarz information criterion (SIC) were used (Gabrielsson and Weiner, 1997).

Fig. 7 *A* shows a semilogarithmic plot of the results derived from the fitting of Eq. 7 to the first set of human bolus intravenous data (Fuite et al., 2002). The inset in Fig.7 *A* represents the fitting results of Eq. 2 to the same data. The values of the optimized parameters are quoted in Table 1. Visual inspection of Fig. 7 *A* and its inset reveals that Eq. 7 can successfully describe these data, whereas this is not the case for the classic MM approach (Eq. 2). The same conclusions can be derived from the analysis of the second set of intravenous data (Skerjanec et al., 1996), which are shown in Fig.7 *B* (for Eq. 7) and at the inset of Fig.7 *B* for Eq. 2. Again, Eq. 7 shows a very good description of the experimental data, whereas the classic MM model fails to describe the data adequately. The parameter estimates for the second set of intravenous data derived after optimization along with the statistical criteria values are listed in Table 1. It should also be noted that these observations agree with the values of the corresponding statistical criteria (AIC, SIC) (see Table 1).

The analytical power of Eqs. 2 and 7 was also tested using mibefradil data obtained after oral administration (Skerjanec et al., 1996; Welker, 1998). To this end, the fitting of Eqs. 2 and 7 was applied only to the data of the declining limb of the concentration-time curve. For both oral data sets examined, the two models described the data correctly (results are not

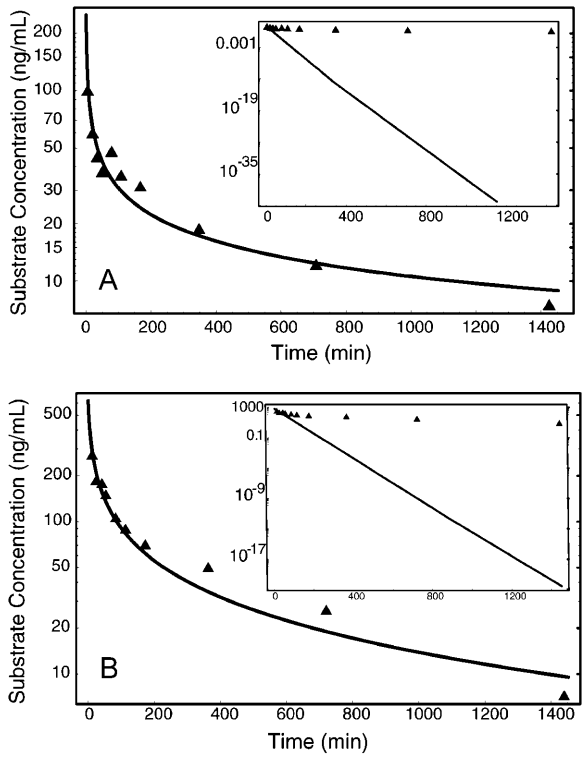

FIGURE 7 Semilogarithmic concentration (p_s) versus time plots of mibefradil after intravenous bolus administration. Data were taken from reference Fuite et al. (2002) (*A*), and reference Skerjanec et al. (1996) (*B*). The solid lines represent the fittings of Eqs. 2 (*A* and *B insets*) and 7 (*A* and *B*) to experimental data.

TABLE 1 Parameter values derived after optimization of two models using experimental and simulated data

Parameter	Data set* (route, reference)					
	i.v. (Fuite et al., 2002)	i.v. (Skerjanec et al., 1996)	p.o. (Skerjanec et al., 1996)	p.o. (Welker, 1998)	sim1†	sim2‡
			Eq. 2			
v^*_{max} (ng/mL/min)	6791.4 (48,366.7)	467.9 (1098.2)	1.03 (0.3)	19.9 (2.9)	222.7 (169.5)	157.1 (10.3)
K_M (ng/mL)	70,215.0 (499,008.0)	12404.9 (29,369.9)	506.4 (172.9)	10,819.6 (1678.7)	36,052.5 (26,024.0)	61,166.2 (32,94.9)
AIC§	97.2	112.1	36.4	30.8	73.0	23.3
SIC¶	97.8	112.7	35.7	30.4	73.8	24.1
			Eq. 7			
v^*_{max} (ng/mL/min)	71.9 (6.5)	88.4 (6.8)	0.824 (0.04)	0.269 (0.05)	1.168 (0.05)	1.029 (0.09)
K_{M0} (ng/mL × (min)$^{-h}$)	154.8 (18.4)	273.4 (38.8)	50.3 (9.1)	2.59 (1.8)	4.681 (0.37)	272.02 (28.8)
h	1.0 (0.0)	0.84 (0.02)	0.325 (0.02)	0.595 (0.04)	0.760 (0.007)	0.0636 (0.03)
AIC§	71.9	83.0	30.9	30.0	33.7	28.9
SIC¶	72.8	83.9	29.7	29.4	34.9	30.1

Values of the statistical criteria applied to the optimization results of the two models.

*The value in parentheses represents standard deviation.

†Simulated data were generated using $k_a = 1.0$ (arbitrary time units)$^{-1}$ to mimic a rapid ''intravenous-like'' drug administration; estimates for v^*_{max}, K_M, and K_{m0} are in arbitrary units.

‡Simulated data were generated using $k_a = 0.01$ (arbitrary time units)$^{-1}$ to mimic oral drug administration; estimates for v^*_{max}, K_M, and K_{m0} are in arbitrary units.

§Akaike information criterion (Gabrielsson and Weiner, 1997).

¶Schwarz information criterion (Gabrielsson and Weiner, 1997).

shown). The estimates of the model parameters and the values of the statistical criteria for the oral data fittings are listed in Table 1 under the two columns with the p.o. sign.

The discrepancy of the fitting results between the intravenous and oral data is associated with the specific kinetic characteristics of the two types of administration. After intravenous bolus administration the entire quantity of drug reaches the liver as a ''bolus'' through the hepatic artery. On the contrary, the drug (substrate) reaches the liver gradually via the portal vein following the rate of uptake after oral administration. Besides, mibefradil exhibits extensive first-pass effect and therefore the portal vein concentration of the gradually absorbed mibefradil is considerably lower than the plasma concentrations of intravenous bolus administration. All these observations substantiate the view that only the i.v. bolus administration creates favorable conditions for the manifestation of fractal kinetics characteristics of the enzyme reaction.

To further verify our physically based interpretation for the differences noted in the analysis of i.v. and oral experimental data, a pharmacokinetic simulation study was undertaken. A model with one-compartment disposition, first-order input and elimination following Eq. 7 was utilized. Two sets of oral data were generated utilizing a high value for the absorption rate constant, $k_a = 1.0$ (arbitrary time units)$^{-1}$ to mimic a rapid ''intravenous-like'' drug administration and a low value for $k_a = 0.01$ (arbitrary time units)$^{-1}$ implementing a slower input rate. Again, Eqs. 2 and 7 were utilized for the analysis of the declining phase data. The fitting results obtained from the simulation data, Fig. 8, were found to be in agreement with the results of the experimental data. The time-dependent MM model (Eq. 7) described nicely both the two sets of data (Fig. 8, *A* and *B*). In contrast, Eq. 2 described the data correctly when a low value was assigned to the absorption rate constant (Fig. 8 *B inset*) and failed to describe the data adhering to the higher input rate (Fig. 8 *A inset*).

A decrease in metabolic clearance with time for certain drugs is usually attributed to self-inhibition (Wolf et al., 1997). However, the manifestation of self-inhibition requires repetitive administration of the drug inhibiting its own metabolism. In this study, the mechanism that caused the time dependency of K_M for mibefradil was attributed to spatial restriction of the in vivo reactions because the reduction in clearance was observed during the time course of a single i.v. bolus administration. To the best of our knowledge, this is the first physically based mechanism proposed for the reduction in metabolic clearance with time. However, a singular observation for the increase of Michaelis constant (K_M) of cyclosporine during the first four months after transplantation (Wolf et al., 1997) has not been elucidated as yet. This mechanism could be proposed, because both the simulation (Berry, 2002) and the experimental results quoted above indicate that the ''time-scale'' for the manifestation of K_M reduction depends on the ''reaction conditions'' (substrate (drug), enzyme, substrate density (dose), route of administration, input rate). In parallel, one should also add that cyclosporine causes hepatic toxicity leading to histological changes that can progressively affect the topological constraints of the reaction space because in vivo reactions occur on membranes or channels of the hepatic cells (Savageau, 1998). It was shown above that the microscopic model and the Monte-Carlo simulations for the enzyme reaction taking place in

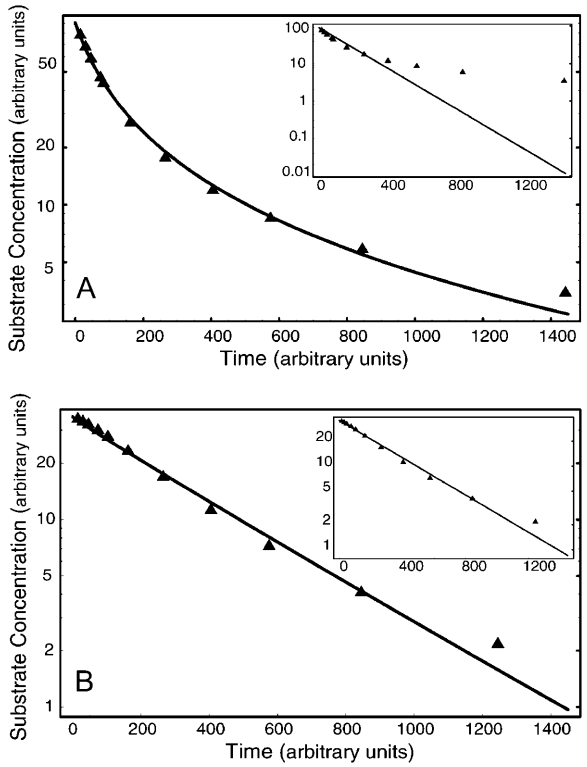

FIGURE 8 Semilogarithmic concentration (p_s) versus time plots for data generated from one-compartment model with first-order input and elimination based on Eq. 7. The parameter values (in arbitrary units) used for the generation of data are: $V_m = 0.4$, $K_{m0} = 0.2$, $h = 1.0$, dose $X_0 = 100$, and either a high 1.0 (*A*) or low 0.01 (*B*) value for the absorption rate constant. The lines represent the fitting results of the two models: classic MM (*A* and *B insets*) and fractal model (*A* and *B*) to data.

a disordered medium can explain the unusual nonlinear pharmacokinetics of mibefradil. These findings allow one to infer that fractal kinetics governs the biotransformation of mibefradil at the microscopic level and this is actually observed at the macroscopic level. Based on the above we propose a novel pharmacokinetic model that provides a more realistic approach than the conventional MM formalism, and it is much simpler to implement than the complete mathematical treatment of Eqs. 3–6. We emphasize once more that the macroscopic model described by Eq. 7 is not supposed to represent the unique approach for the description of anomalous MM kinetics. However, Eq. 7 was not derived empirically but it was based on our MC simulations.

This work was supported by the General Secretariat of Research and Technology of Greece (PENED grant 70/3/6508).

REFERENCES

Agutter, P., P. Malone, and D. Wheatley. 1995. Intracellular transport mechanism: a critique of diffusion theory. *J. Theor. Biol.* 176:261–272.

Argyrakis, P., R. Kopelman, and K. Lindenberg. 1993. Diffusion-limited binary reactions: the hierarchy of nonclassical regimes for random initial conditions. *Chem. Phys.* 177:85032–85034.

Berry, H. 2002. Monte Carlo simulations of enzyme reactions in two dimensions: fractal kinetics and spatial segregation. *Biophys. J.* 83:1891–1901.

Bonny, J. D., and H. Leuenberger. 1991. Matrix type controlled release systems. I. Effect of percolation on drug dissolution kinetics. *Pharm. Acta Helv.* 66:160–164.

Bonny, J. D., and H. Leuenberger. 1993. Matrix type controlled release systems. II. Percolation effects in non-swellable matrices. *Pharm. Acta Helv.* 68:25–33.

Frauenfelder, H., P. Wolynes, and R. Austin. 1999. Biological physics. *Rev. Mod. Phys.* 71:S419–S430.

Fuite, J., R. Marsh, and J. Tuszynski. 2002. Fractal pharmacokinetics of the drug mibefradil in the liver. *Phys. Rev. E. Stat. Nonlin. Soft. Matter. Phys.* 66:021904.

Gabrielsson, J., and D. Weiner. 1997. Pharmacokinetic and Pharmacodynamic Data Analysis: Concepts and Applications. Swedish Pharmaceutical Press, Stockholm, Sweden.

Hoshen, J., and R. Kopelman. 1976. Percolation and cluster distribution. I. Cluster multiple labeling technique and critical concentration algorithm. *Phys. Rev. B.* 1:3438–3445.

Javanaud, C. 1989. The application of a fractal model to the scattering of ultrasound in biological media. *J. Acoust. Soc. Am.* 86:493–496.

Koo, Y.-E. L., and R. Kopelman. 1991. Space- and time-resolved diffusion-limited binary reaction kinetics in capillaries. Experimental observation of segregation, anomalous exponents and depletion zone. *J. Stat. Phys.* 65:893–918.

Kopelman, R. 1988. Fractal reaction kinetics. *Science.* 241:1620–1626.

Köpf, M., C. Corinth, O. Haferkamp, and T. F. Nonnenmacher. 1996. Anomalous diffusion of water in biological tissues. *Biophys. J.* 70:2950–2958.

Kosmidis, K., P. Argyrakis, and P. Macheras. 2003a. A reappraisal of drug release laws using Monte Carlo simulations: the prevalence of the Weibull function. *Pharm. Res.* 20:988–995.

Kosmidis, K., P. Argyrakis, and P. Macheras. 2003b. Fractal kinetics in drug release from finite fractal matrices. *J. Chem. Phys.* 119:6373–6377.

López-Quintela, M., and J. Casado. 1989. Revision of the methodology in enzyme kinetics: a fractal approach. *J. Theor. Biol.* 139:129–139.

Luby-Phelps, K., P. Castle, D. Taylor, and F. Lanni. 1987. Hindered diffusion of inert tracer particles in the cytoplasm of mouse 3T3 cells. *Proc. Natl. Acad. Sci. USA.* 84:4910–4913.

Macheras, P. 1995. Carrier-mediated transport can obey fractal kinetics. *Pharm. Res.* 12:541–548.

Michaelis, L., and M. L. Menten. 1913. Die kinetik der invertinwirkung. *Biochem. Z.* 49:333–369.

Minton, A. P. 1993. Macromolecular crowding and molecular recognition. *J. Mol. Recognit.* 6:211–214.

Minton, A. P. 1998. Molecular crowding: analysis of effects of high concentrations of inert cosolutes on biochemical equilibria and rates in terms of volume exclusion. *Methods Enzymol.* 295:127–149.

Montroll, E. W., and G. H. Weiss. 1965. Random walks on lattices. II. *J. Math. Phys.* 6:167–181.

Murray, J. D. 1993. Mathematical Biology. Springer-Verlag, New York.

Ogihara, T., I. Tamai, and A. Tsuji. 1998. Application of fractal kinetics for carrier-mediated transport of drugs across intestinal epithelial membrane. *Pharm. Res.* 15:620–625.

Press, W., B. Flannery, S. Teukolsky and W. Vetterling. 1988. Numerical Recipes, Cambridge University Press, Cambridge, UK.

Ramakrishnan, A., and A. Sadana. 2002. A mathematical analysis using fractals for binding interactions of nuclear estrogen receptors occurring on biosensor surfaces. *Anal. Biochem.* 303:78–92.

Sadana, A. 2001. A kinetic study of analyte-receptor binding and dissociation, and dissociation alone, for biosensor applications: a fractal analysis. *Anal. Biochem.* 291:34–47.

Savageau, M. 1998. Development of fractal kinetic theory for enzyme-catalysed reactions and implications for the design of biochemical pathways. *Biosystems*. 47:9–36.

Scalettar, B., J. Abney, and C. Hackenbrock. 1991. Dynamics, structure, and functions are coupled in the mitochondrial matrix. *Proc. Natl. Acad. Sci. USA*. 88:8057–8061.

Schwille, P., J. Korlach, and W. Webb. 1999. Fluorescence correlation spectroscopy with single-molecule sensitivity on cell and model membranes. *Cytometry*. 36:176–182.

Skerjanec, A., S. Tawfik, and Y. Tam. 1996. Nonlinear pharmacokinetics of mibefradil in the dog. *J. Pharm. Sci*. 85:189–192.

Wachsmuth, M., W. Waldeck, and J. Langowski. 2000. Anomalous diffusion of fluorescent probes inside living cell nuclei investigated by spatially-resolved fluorescence correlation spectroscopy. *J. Mol. Biol*. 298:677–689.

Wagner, J. G. 1993. Pharmacokinetics for the Pharmaceutical Scientist, Technomic Publishing Company, Lancaster, PA.

Welker, H. 1998. Single- and multiple-dose mibefradil pharmacokinetics in normal and hypertensive subjects. *J. Pharm. Pharmacol*. 50:983–987.

Wolf, A., C. F. Trendelenburg, C. Diez-Fernandez, P. Prieto, S. Houy, W. E. Trommer, and A. Cordier. 1997. Cyclosporine A-induced oxidative stress in rat hepatocytes. *J. Pharmacol. Exp. Ther*. 280:1328–1334.